Proc. Indian Acad. Sci. (Earth Planet. Sci.), Vol. 104, No. 3, September 1995, pp. 373–383.

Side-stepping of axial surface traces in superposed folding

S K GHOSH

Department of Geological Sciences, Jadavpur University, Calcutta 700 032, India

Abstract. During the refolding of an early non-isoclinal fold (say, F_1) we may find an offset or side-stepping of the axial surfaces of the later folds (say, F_2). The offsets can be seen in both type 2 and type 3 interference patterns. An analysis of the shear fold model shows that there is a maximum limit for the magnitude of side-stepping. The side-stepping is larger for larger interlimb angles of F_1. It decreases with progressive tightening of F_2. By recognizing such side-stepping we can predict on which side the F_1 hinge should lie even if the hinge is unexposed or lies outside the domain of observation. The general rule for the sense of side-stepping is the same for shear folds, flexural slip folds and buckling folds. However, the side-stepping in buckling folds should be used with caution, since F_2 folds on buckled single-layers may show an offset whose sense is opposite to that predicted by the general rule.

Keywords. Superposed folding; axial surfaces; side-stepping.

1. Introduction

During the coaxial folding of an early non-isoclinal fold (say, F_1) we may find an offset or side-stepping of the axial surfaces of the late folds (say, F_2). This feature, first described by Ramsay (1967, p. 509) and Ramsay and Huber (1987) is readily explained by the model of shear folding (Ramsay 1967). In the following analysis this model is discussed in detail with a view to determine the magnitude and sense of side-stepping of axial surfaces of F_2 when the initial shape of the F_1 fold and the nature of variation of the heterogeneous shear across it are given. The sense of side-stepping of flexural slip folds can also be determined by geometrical constructions or by paper stack models. For buckle folds, however, a kinematic model is inadequate, and the sense of side-stepping can only be determined from physical models.

2. Model of shear folding

Let us assume that the limbs of F_1 are straight and that the shear direction for the second deformation is perpendicular to the axial trace of F_1 on its profile plane. In the following analysis it has been further assumed that the magnitude of heterogeneous simple shear varies sinusoidally to generate the F_2 fold (figure 1). The sinusoidal variation of simple shear is shown in figure 1 by the curved axial surface (dashed line) of the deformed F_1 fold. Consider the transverse profile of an early fold (F_1) with axial surface trace parallel to the y co-ordinate axis, with its amplitude a and with two limbs A and B at angles of θ_1 and θ_2 with the x axis (figure 2). The variation of the heterogeneous simple shear of the second deformation can be represented by the

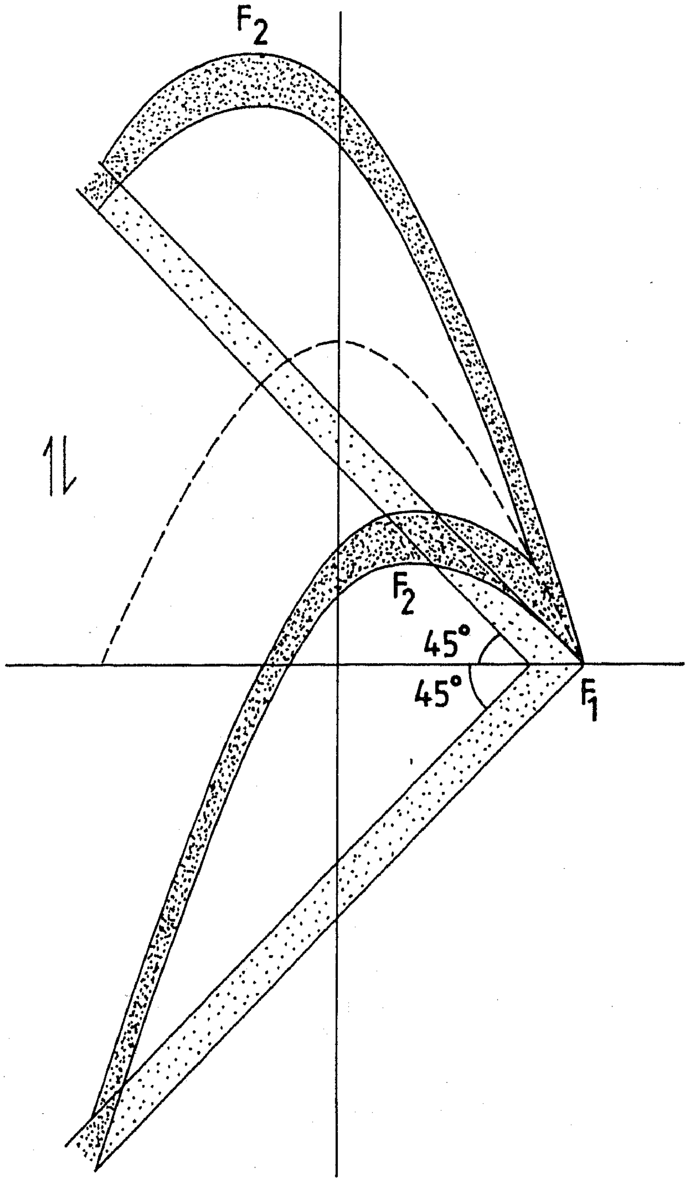

Figure 1. Development of F_2 by shear folding of F_1. The axial trace of F_1 is deformed (dashed line) by sinusoidally varying simple shear. The axial surface traces of the F_2 folds show a left-stepping or sinistral offset if we look across the axial trace of F_1.

equation

$$\gamma = \gamma_0 \sin ly, \tag{1}$$

where $l = 2\pi/\lambda$. For a simple situation it is assumed that $\lambda = 4a$ (figure 2). The F_1 axial surface trace can be represented by the equation

$$x = 0.$$

By simple shear, with the particle-path equation

$$x' = x + \gamma y$$

$$y' = y,$$

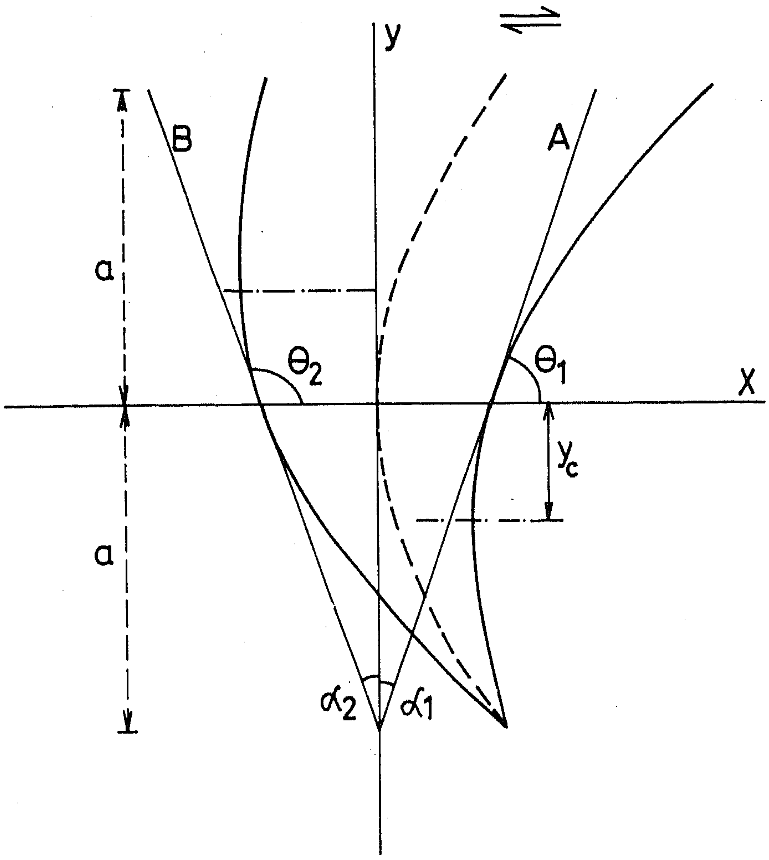

Figure 2. Deformation of F_1 with limbs A and B by dextral shear. The offset of the hinge points of F_2 is y'_c in opposite directions on either side of the hinge point of the deformed axial trace of F_1. The total offset is $2y'_c$.

the axial trace of F_1 is deformed to a curve

$$x' = y'\gamma_0 \sin ly'. \tag{2}$$

Similarly, if the limb A of F_1 is represented by the equation

$$y = x \tan\theta_1 - a,$$

by simple shear it is deformed to the curve

$$x' = y' \cot\theta_1 + \gamma_0 y' \sin ly' + a \cot\theta_1. \tag{3}$$

The F_2 hinge is located where $dx'/dy' = 0$, or

$$ly' \cos ly' + \sin ly' = -\frac{\cot\theta_1}{\gamma_0}.$$

Since,

$$\theta_1 = 90° - \alpha_1$$

$\theta_2 = 90° + \alpha_2$ (figure 2), we have

$$ly' \cos ly' + \sin ly' = -\frac{\tan\alpha_1}{\gamma_0}, \tag{4}$$

$$ly' \cos ly' + \sin ly' = \frac{\tan\alpha_2}{\gamma_0}. \tag{5}$$

For specific values of α_1 and γ_0, each of these equations is satisfied for a particular value of y' (say, y'_c). This is the y-coordinate of the hinge of F_2. For $\alpha_1 = \alpha_2 = 20°$, the y'-coordinate of the hinge is represented (figure 3) in non-dimensional form by the ratio

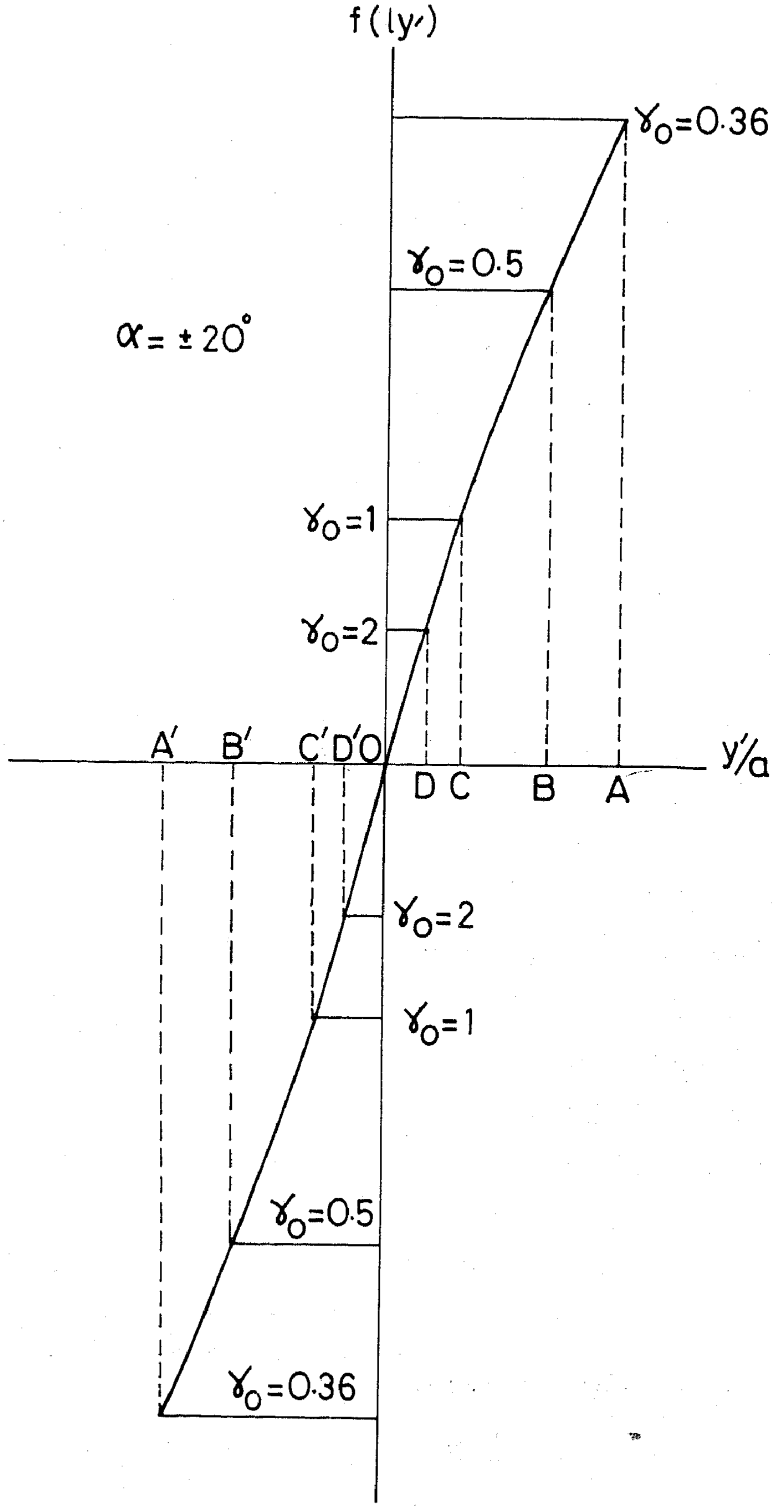

Figure 3. Variation of $f(ly')$ with y'/a for $\alpha = 20°$ for different values of γ_0. The total offsets for $\gamma_0 = 0{\cdot}36$, $0{\cdot}5$, $1{\cdot}0$ and $2{\cdot}0$ are AA', BB', CC' and DD'.

y'/a. Figure 3 shows the variation of $f(ly')$ with y'/a, where $f(ly')$ represents the function on the left hand side of equation (4) or (5). OA and OA' or OB or OB' are the offsets of the F_2 axial surface traces on either side. y'_c has opposite signs for the two limbs because the positions of the hinge points of F_2 are shifted towards opposite directions. The difference between the y'_c values of the two limbs gives us the magnitude of offset. Thus, for example, the total offsets in figure 3 are AA', BB', CC' and DD' with increasing γ_0.

Say, $\alpha_1 = \alpha_2 = \alpha$, so that the interlimb angle of the early fold is 2α. The total offset of the axial surface trace, in nondimensional form, is then $2y'_c/a$. Equations (4) and (5) show that for the same value of γ_0, the magnitude of the total offset increases with an increase of the initial interlimb angle of the early fold (figure 4). For the same value of the interlimb angle of F_1, the offset of axial surface traces of F_2 decreases as these folds are tightened with progressive simple shear (figure 5). In this model of development of F_2 by heterogeneous simple shear the axial surface traces of the F_2 folds are parallel to the direction of simple shear. At the hinge point of F_2 the trace of the limb of F_1 must be rotated to become perpendicular to the direction of simple shear (figures 1, 2 and 5). This may not be possible if the magnitude of simple shear is too small (figure 5a). In other words, if the simple shear is too small the axial surfaces of F_2 do not become well-defined.

There is a maximum limit of the magnitude of side-stepping (y'_c). This limit is obtained from the condition

$$\frac{\mathrm{d}f(ly')}{\mathrm{d}(ly')} = 0,$$

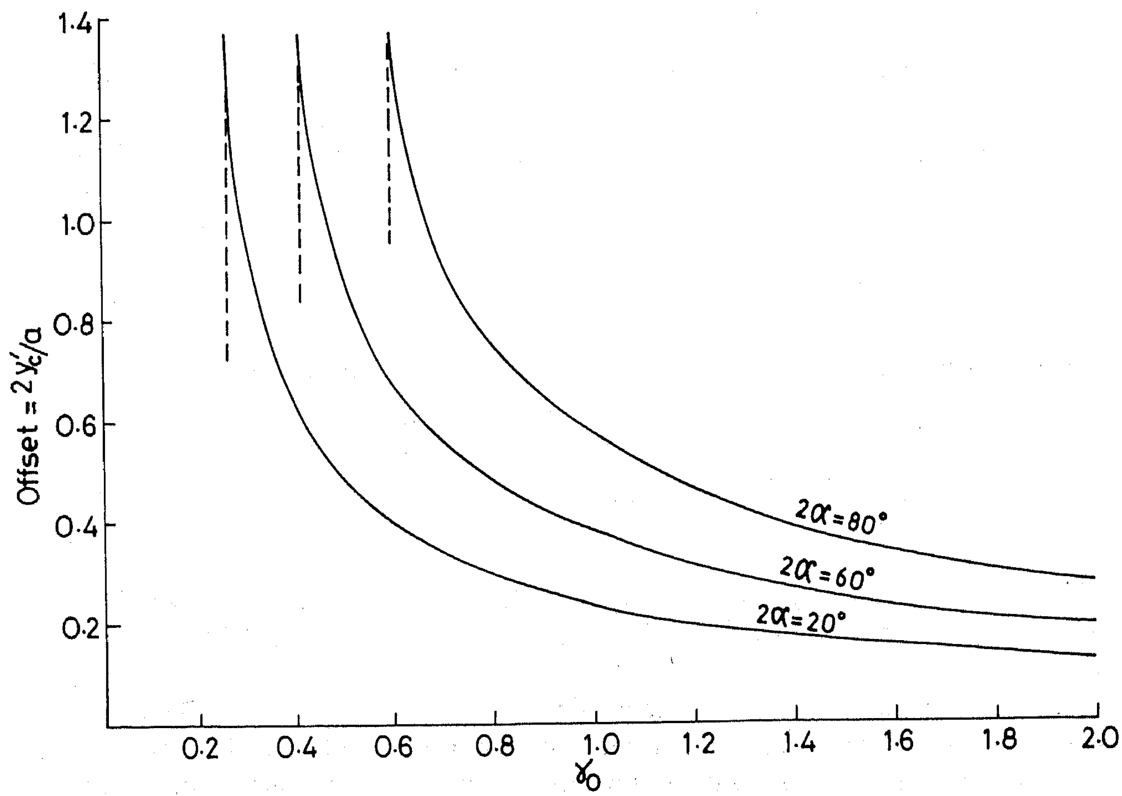

Figure 4. Variation of total offsets $2y'_c/a$ with increasing γ_0 for three interlimb angles, 40°, 60° and 80°, of the initial F_1 fold.

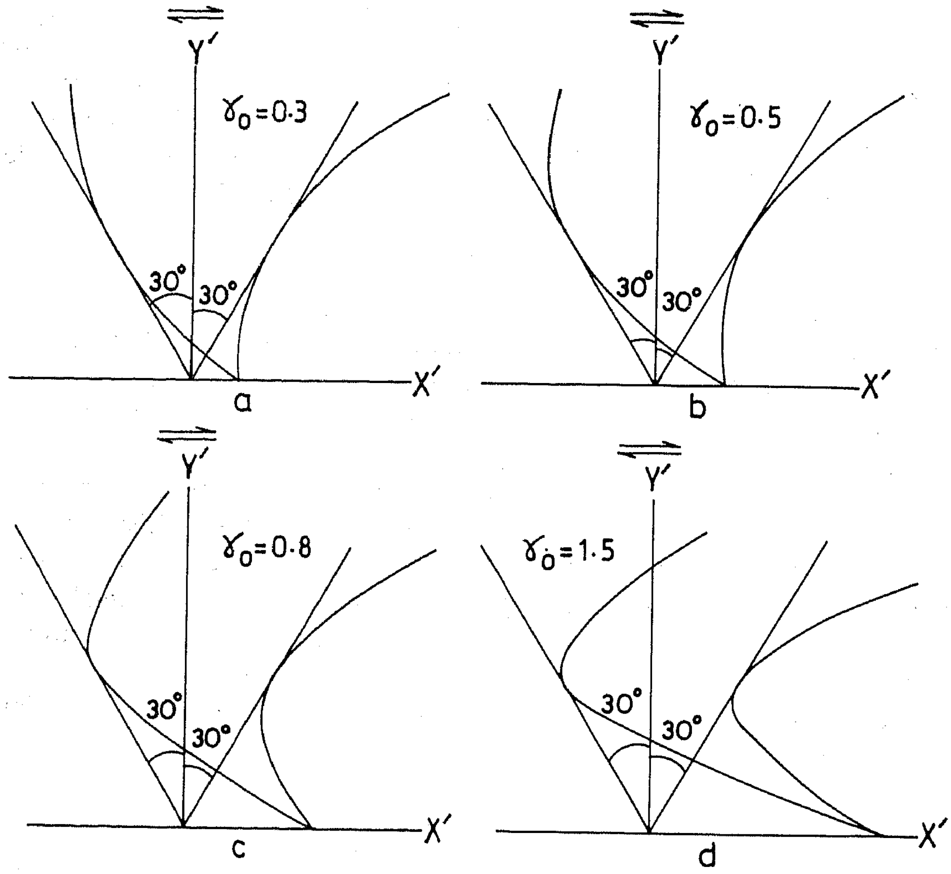

Figure 5. Offset of hinge points of F_2 folds produced by shear folding of a F_1 fold. Each of two limbs of the F_1 fold make an angle of 30° with the axial trace parallel to y. Note that if γ_0 is too small, as in figure 5a, the limbs of F_1 are not significantly rotated to make the hinge parallel to y.

where $f(ly')$ represents the left hand side of equation (4) or (5). From this condition we obtain the relation

$$\tan ly' = \frac{2}{ly'}. \tag{6}$$

The solution of this equation can be obtained graphically from the intersection of the curves

$$z = \tan ly', \text{ and}$$
$$z = 2/(ly'). \tag{7}$$

The maximum value of y_c'/a is 0·685 (figure 6). In other words, the largest possible total offset $(2y_c'/a)$ of the axial traces of F_2 is 1·37, irrespective of the interlimb angle of F_1 (dotted line in figure 4).

The idealized model of heterogeneous simple shear gives us the following rule for the sense of side-stepping of the F_2 axial traces. If we move across the axial trace of F_1, with the F_1 hinge on the left hand side, an upward closing F_2 fold will show a right-stepping or a dextral shift (figure 7a) and a downward closing F_2 fold will show a left-stepping (figure 7c). If we look across the axial trace of F_1, with the F_1 hinge on our right, an

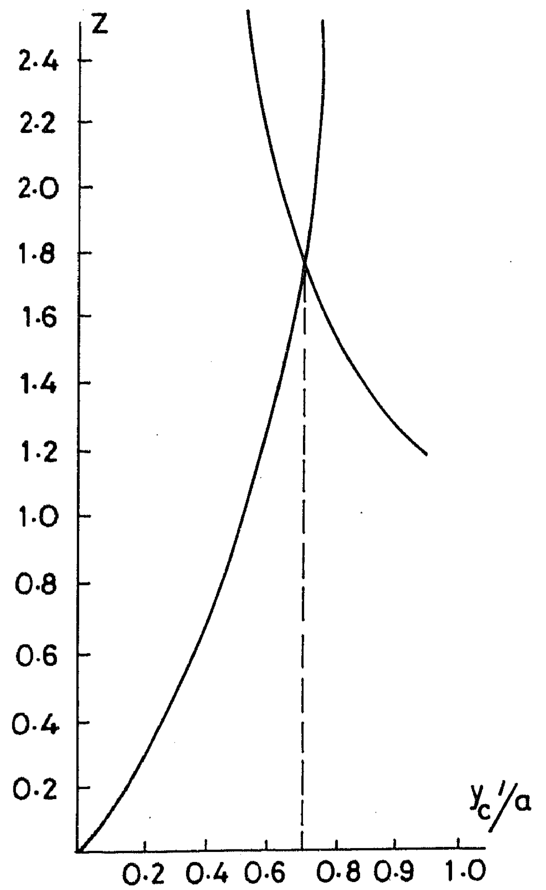

Figure 6. Determination of maximum value of y_c'/a from intersection of two curves.

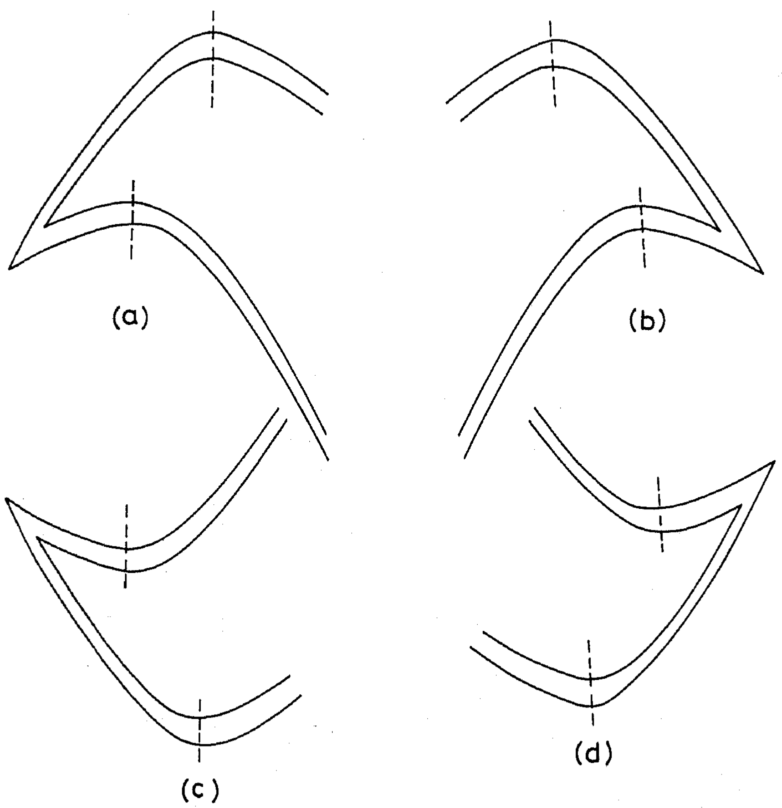

Figure 7. Rule of axial trace offset of F_2 folds produced by heterogeneous shear.

upward closing F_2 will show a left-stepping (figure 7b) and a downward closing F_2 will show a right-stepping (figure 7d).

3. Side-stepping of axial surfaces in other types of folds

Natural folds are mostly buckling folds or flexural slip folds. From both paper stack models and graphical construction (figure 8), it is found that there is a side-stepping of axial surfaces of second generation flexural slip folds if the first generation fold is non-isoclinal. Figure 8a shows the transverse profile of an initial F_1 fold with horizontal traces of the axial plane cleavage. In figure 8b a parallel fold has been geometrically constructed on the cleavage traces, with the assumption that the deformation was by the ideal model of flexural flow (Ramsay and Huber 1987). The shape of the deformed bedding is constructed by measuring the arc-length distances of points on the bedding traces from the hinge point along several cleavage traces parallel to AB, CD or EF (figure 8b). Evidently, these arc-length distances remain the same in the deformed and undeformed models (figures 8a and 8b). The rule concerning the sense of side-stepping is the same as in the case of shear folding. The magnitude of side-stepping increases with an increase in the initial interlimb angle of F_1. It decreases with progressive tightening of F_2.

Unlike the idealized models of shear folding and flexural slip folding, the modification of earlier folds by buckling (Ghosh 1993, p. 337) cannot be analysed by a kinematic model. To get an insight into this problem, experiments on coaxial refolding were carried out with soft models of multilayers and single layers of the same types as described by Ghosh *et al* (1992, 1993). The first generation folds in these models were tight but not isoclinal. The models were deformed by pure shear, with the direction of

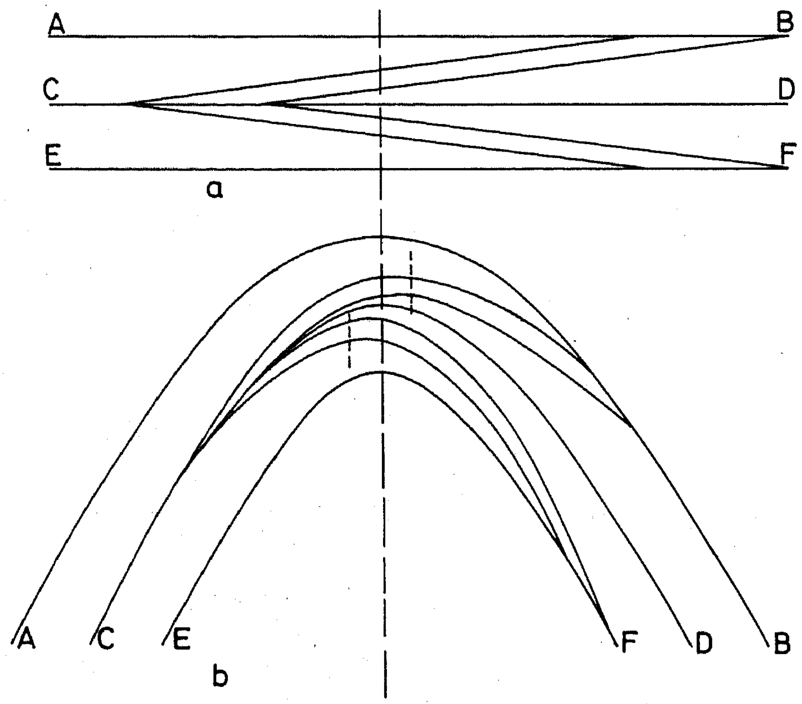

Figure 8. Geometrical construction to show offset of F_2 axial surfaces by flexural slip folding.

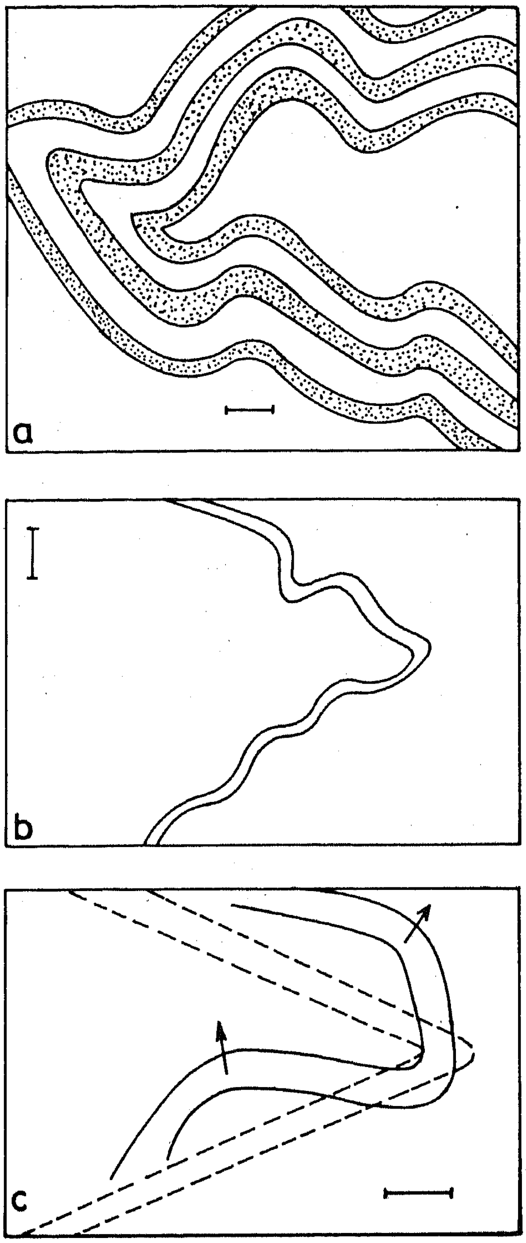

Figure 9. Sections of models showing superposed buckling. F_1 and F_2 are coaxial. (**a**) Offset of axial surface traces of F_2 folds in experiment of superposed buckling of a multilayer. Dotted layers and the intervening blank layers are modelling clay with greased interfaces. The rest of the blank areas are of painter's putty. (**b**) Superposed buckling in single layer of modelling clay embedded in painter's putty. Note that the side-stepping of axial surface traces has a sense opposite to that shown by the shear fold models. (**c**) Superposed buckling in a thin multilayer of a few layers of modelling clay. The embedding medium is painter's putty. Note the sense of axial trace offsets of F_2 folds. The hinge of each F_2 fold tends to move along a direction at a high angle to the trends of the F_1 limbs (scale bars 1 cm).

shortening parallel to the axial planes of F_1 and perpendicular to the F_1 axis. The second generation buckling folds in the thick multilayered models showed on the profile plane a side-stepping of axial surface traces (figure 9a) in the same sense as in the shear fold model. In the other set of experiments the F_1 folds were produced on single layers of modelling clay or on thin multilayers embedded in painter's putty. During the second stage of deformation, with the direction of shortening parallel to the axial plane of F_1 and perpendicular to the F_1 axis, the axial planes of F_2 were not at a right angle to the direction of the second shortening. In the initial stage of the second deformation, the axial surface trace of an F_2 fold on the profile plane was at a high angle to the traces of the F_1 fold limbs so that the axial surfaces of F_2 folds, produced on the two limbs of an F_1 fold, were not parallel (figures 9b, 9c). With progressive deformation, the angle between the axial surfaces of the two F_2 folds was reduced and both surfaces made lower angles with the XY plane of the second deformation. Yet, the two F_2 axial surfaces remained non-parallel even at a large value of bulk shortening. If we look along the trace of the XZ plane on the fold profile, the hinges of the two F_2 folds show sidewise shifting with respect to each other, and the sense of this shifting is opposite to that of the model of shear folding.

Side-stepping of F_2 axial surface traces is not restricted to the type 3 interference. In experiments of superposed buckling of multilayers, offsets of F_2 axial traces are often seen in model sections of a type 2 fold interference when the traces of limbs of F_1 folds are not parallel (figure 10). Figure 10 shows the outcrop pattern on the horizontal section of a part of a multilayered model which had undergone superposed buckling, with the direction of second shortening parallel to the axis of the first generation folds. The sense of side-stepping of the F_2 axial traces is in accordance with the general rule as given above, although an opposite sense of offset can be seen in some places. Thus, in the outcrop of the thick layer of modelling clay (dotted) the axial trace offsets of F_2 are in agreement with the general rule. However, in the thin layer (black) the offset of F_2 axial traces is opposite to the general rule on the right side of the figure near the downward closing nose of the F_1 fold. It is suggested that during disharmonic buckle folding a competent layer within a multilayer may deform in certain segments more or less independently as a single unit. The sense of side-stepping of axial traces of buckle folds should therefore be used with some caution.

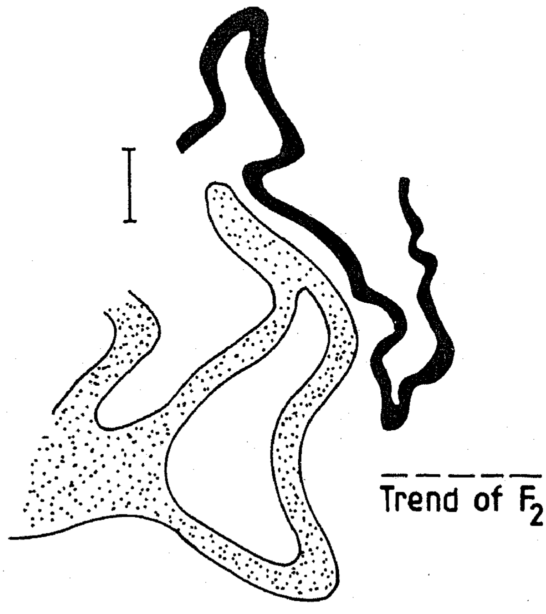

Figure 10. Horizontal section of multilayered model showing two generations of disharmonic buckle folds. Only a part of the model is shown. The fold interference pattern is of type 2. Note the sense of offset of axial traces of F_2 folds (scale bar 1 cm).

4. Conclusion

The offset of axial surface traces is a useful feature for structural analysis of both type 3 and type 2 fold interferences. In areas of superposed folding it is often difficult to locate or identify the hinges of early folds. Moreover, when the early fold is tight and has a large amplitude it may not be possible to distinguish its different limbs if later folds are superimposed on them. From the axial trace offsets we may then identify the presence of two generations of folds even if the early fold hinge is not located in the outcrop. It may also be possible to locate the axial surface trace of the early fold either in outcrop scale or in the map scale, even if the early fold closure lies outside the observed domain. The analysis given above shows that, from the magnitude of offset and the tightness of the F_2 folds, we may obtain an approximate idea of the initial tightness of F_1. Large offsets are expected when F_2 is fairly open and F_1 is moderately tight. Evidently, offsets of F_2 axial traces should not occur if F_1 was strictly isoclinal. From the sense of offset we can determine on which side of the F_2 axial surface the F_1 hinge is situated. The model of shear folding shows that there is a maximum limit for the value of side-stepping. The sense of side-stepping for flexural slip folds and buckle-folded multilayers is, in general, the same as in the model of shear folding; the sense of side-stepping in single-layer buckle folds may, however, be the opposite.

References

Ghosh S K 1993 *Structural Geology: Fundamentals and Modern Developments* (Oxford: Pergamon Press) 598 pp

Ghosh S K, Mandal N, Khan D and Deb S 1992 Modes of superposed buckling in single layers controlled by initial tightness of early folds; *J. Struct. Geol.* **14** 381–394

Ghosh S K, Mandal N, Sengupta Sudipta, Deb S and Khan D 1993 Superposed buckling in multilayers; *J. Struct. Geol.* **15** 95–111

Ramsay J G 1967 *Folding and Fracturing of Rocks* (New York: McGraw-Hill) 568 pp

Ramsay J G and Huber M I 1987 *The Techniques of Modern Structural Geology. 2. Folds and Fractures.* (London: Academic Press) 307 pp